The Journal of Neuroscience, August 15, 2001, 21(16):6283–6291

The Inferior Parietal Lobule Is the Target of Output from the Superior Colliculus, Hippocampus, and Cerebellum

Dottie M. Clower,[1,2] Robert A. West,[3] James C. Lynch,[4] and Peter L. Strick[1,2]

[1]Research Service, Veterans Administration Medical Center, Pittsburgh, Pennsylvania 15261, [2]Departments of Neurobiology, Neurological Surgery, and Psychiatry and Center for the Neural Basis of Cognition, University of Pittsburgh, Pittsburgh, Pennsylvania 15261, [3]Department of Physiology, State University of New York Health Science Center at Syracuse, and Central New York Research Corporation, Syracuse Veterans Affairs Medical Center, Syracuse, New York 13210, and [4]Departments of Anatomy, Ophthalmology, and Neurology, University of Mississippi Medical Center, Jackson, Mississippi 39216

The inferior parietal lobule (IPL) is a functionally and anatomically heterogeneous region that is concerned with multiple aspects of sensory processing and sensorimotor integration. Although considerable information is available about the corticocortical connections to the IPL, much less is known about the origin and importance of subcortical inputs to this cortical region. To examine this issue, we used retrograde transneuronal transport of the McIntyre-B strain of herpes simplex virus type 1 (HSV1) to identify the second-order neurons in subcortical nuclei that project to the IPL. Four monkeys (*Cebus apella*) received injections of HSV1 into three different subregions of the IPL. Injections into a portion of the lateral intraparietal area labeled second-order neurons primarily in the superficial (visual) layers of the superior colliculus. Injections of HSV1 into a portion of area 7a labeled many second-order neurons in the CA1 region of the hippocampus. In contrast, virus injections within a portion of area 7b labeled second-order neurons in posterior regions of the dentate nucleus of the cerebellum. These observations have some important functional implications. The IPL is known to be involved in oculomotor and attentional mechanisms, the establishment of maps of extrapersonal space, and the adaptive recalibration of eye–hand coordination. Our findings suggest that these functions are subserved by distinct subcortical systems from the superior colliculus, hippocampus, and cerebellum. Furthermore, the finding that each system appears to target a separate subregion of the IPL provides an anatomical substrate for understanding the functional heterogeneity of the IPL.

Key words: posterior parietal cortex; LIP; area 7a; area 7b; dentate nucleus; oculomotor

The inferior parietal lobe (IPL) is thought to be involved in a diverse set of neural operations, including spatial attention, multimodal sensory integration, and oculomotor control (Lynch, 1980; Hyvarinen, 1981). Electrophysiological studies have demonstrated that neurons in IPL have response properties ranging from attention-enhanced visual and oculomotor responses (Lynch et al., 1977; Goldberg et al., 1990; Colby et al., 1996) to complex patterns of activity during object visualization and manipulation (Sakata et al., 1995; Murata et al., 1996). Some of these properties have led to the concept that IPL participates in building multiple spatial representations for the guidance of both eye and limb movements (Andersen, 1989; Colby and Goldberg, 1999).

Anatomical evidence indicates that IPL is a heterogeneous structure, with subregions characterized by unique patterns of cortical and subcortical connections (Pandya and Seltzer, 1982; Asanuma et al., 1985; May and Andersen, 1986; Cavada and Goldman-Rakic, 1989a,b, 1991; Andersen et al., 1990; Lewis and Van Essen, 2000). For example, the lateral intraparietal area (LIP) is extensively interconnected with the frontal eye field (FEF), as well as with other visual cortical areas, and projects heavily to the intermediate layers of the superior colliculus (Barbas and Mesulam, 1981; Lynch et al., 1985; Andersen et al., 1990). Another subregion of IPL, area 7b, is preferentially connected to somatosensory areas I and II and the ventral premotor area (PMv) (Cavada and Goldman-Rakic, 1989a,b; Andersen et al., 1990). A third subregion of IPL, area 7a, shows little connectivity to FEF and no projection to the superior colliculus (Lynch et al., 1985; Andersen et al., 1990); yet area 7a has stronger connectivity to the dorsolateral prefrontal cortex than has either LIP or area 7b (Cavada and Goldman-Rakic, 1989b). It is likely that the functional subdivisions in IPL reflect, in part, this differential connectivity.

Little is known about the subcortical inputs to different subregions of IPL. Thalamic inputs to LIP, area 7a, and area 7b are known to be distinct (Asanuma et al., 1985; Schmahmann and Pandya, 1990; Hardy and Lynch, 1992). Such segregation of the thalamic projections suggests that the subdivisions of IPL receive unique patterns of subcortical inputs as well. However, the disynaptic nature of these connections has made it difficult to define these pathways. Therefore, we used retrograde transneuronal transport of the McIntyre-B strain of herpes simplex virus type 1 (HSV1) to determine subcortical inputs to portions of LIP, area 7a, and area 7b. There are two major results of this study. First, we found that the IPL is the target of disynaptic outputs from the superior colliculus, hippocampus, and cerebellum. Second, each of these subcortical nuclei projects to a different subregion of the IPL.

Received Dec. 22, 2000; revised May 9, 2001; accepted May 15, 2001.

This work was supported by the Veterans Affairs Medical Research Service (P.L.S.) and by United States Public Health Service Grant MH56661 (P.L.S.) and the Joe Weinberg Research Fund (J.C.L.). We thank M. Page for the development of computer programs and K. Hughes and M. O'Malley-Davis for their expert technical assistance. We also thank Drs. D. I. Bernstein (Children's Hospital Medical Center, Cincinnati, OH) and R. D. Dix (Jones Eye Institute, University of Arkansas for Medical Sciences, Little Rock, AR) for supplying HSV1.

D.M.C. and R.A.W. contributed equally to this work.

Correspondence should be addressed to Dr. Peter L. Strick, University of Pittsburgh, W1640 Biomedical Science Tower, 200 Lothrop Street, Pittsburgh, PA 15261. E-mail: strickp@pitt.edu.

Parts of this paper have been published previously in abstract form (West et al., 1998, 1999).

MATERIALS AND METHODS

This report is based on observations from four juvenile *Cebus apella* monkeys. The McIntyre-B strain of HSV1 was injected into different portions of the inferior parietal cortex in four hemispheres. This strain of HSV1 travels transneuronally in the retrograde direction in a time-dependent manner (Zemanick et al., 1991; Strick and Card, 1992; Hoover and Strick, 1999). The procedures adopted for this study and the care provided experimental animals conformed to the regulations detailed in the *National Institutes of Health Guide for the Care and Use of Laboratory Animals*. All protocols were reviewed and approved by the Institutional Animal Care and Use committees. The biosafety precautions taken during these experiments conformed to or exceeded biosafety level 2 (BSL-2) regulations detailed in *Biosafety in Microbiological and Biomedical Laboratories* (Health and Human Services Publication 93-8395). A detailed description of the procedures for handling virus and virus-infected animals is presented in Strick and Card (1992) and Hoover and Strick (1999).

Surgery. Twelve hours before surgery, each animal was administered dexamethasone (Decadron, 0.5 mg/kg, i.m.) and restricted from food and water. Approximately twenty minutes before anesthesia was initiated, animals were pretreated with either atropine sulfate (0.05 mg/kg, i.m.) or glycopyrrolate (0.01 mg/kg, i.m.). Most of the animals were anesthetized initially with ketamine hydrochloride (Ketalar, 15–20 mg/kg, i.m.), intubated, and maintained under gas anesthesia using a 1:1 mixture of isoflurane (Enflurane) and nitrous oxide (1.5–2.5%; 1–3 l/min). Other animals were anesthetized with Telazol (initial dose, 20 mg/kg, i.m.; supplemental dose, 5–7 $mg \cdot kg^{-1} \cdot hr^{-1}$, i.m.). In these cases, the analgesic butorphenol (Torbugesic, 0.1–0.4 mg/kg, i.m.) was given every 2–4 hr to reduce the overall amount of Telazol used. After being anesthetized, all animals were administered dexamethasone (0.5 mg/kg, i.m.) and an antibiotic [cefazolin sodium (Kefzol, 25 mg/kg, i.m.) or ceftriaxone (Rocephin, 75 mg/kg, i.m.)]. Hydration was maintained using lactated Ringer's solution with 5% dextrose (6–10 cc/hr, i.v.), and temperature was maintained with a heating pad. Heart rate, blood oxygen saturation, body temperature, and respiratory depth were continuously monitored during the surgery.

All surgical procedures were conducted using aseptic techniques. Each animal's head was positioned in a stereotaxic frame (Kopf). Ophthalmic ointment was placed in the eyes. A craniotomy was performed over the parietal lobe, and the dura was incised and reflected to expose the region of interest. The cortex was kept moist by the use of warmed (37–40°C) sterile saline throughout the entire procedure.

Injection sites. One monkey received injections into LIP as well as portions of area 7a and area 7b. The other monkeys received smaller injections focused within one of the above-mentioned subregions. The location of each injection site was based on surface landmarks and their known relationship to the cytoarchitectonic borders of parietal cortex. LIP has been defined as a region in the lateral or posterior bank of the intraparietal sulcus that projects to the FEF (Andersen et al., 1985). A previous anatomical study confirmed that LIP occupies a similar location in the *Cebus* monkey (Tian and Lynch, 1996).

To guide the HSV1 injections visually into the posterior bank of the intraparietal sulcus, in some animals we removed the medial bank of the parietal sulcus using subpial aspiration. We then used a 5 μl Hamilton syringe with a 28–32 gauge removable needle to place multiple injections (0.2 μl per site) of virus into selected regions of the inferior parietal cortex (see Fig. 1). For injections into the intraparietal sulcus, the tip of the needle was bent at a 90° angle to insure injections were made normal to the cortical surface. The depth of the injections was designed to place the tip of the syringe needle in cortical layer IV. Injections were spaced 1 mm apart except to avoid blood vessels. The absolute number of injections in each animal varied according to the size of the targeted region (see Fig. 1). After each injection into the cortex, the needle remained in place for 1–3 min. When the injections were completed, the dura was sutured (if possible), the bone flap was replaced and fixed with sheets of SILASTIC, and the wound was closed in anatomical layers.

Survival period. After the surgery, animals were placed in a BSL-2 isolation room for further observation and recovery. Observations of each animal's appearance and behavior were recorded every 4–8 hr, or more often as needed. All animals received dexamethasone (0.1–0.5 mg/kg, i.m. or p.o.) during the initial recovery period. Animals that showed signs of discomfort were given butorphenol (0.01–0.4 mg/kg, i.m.) or buprenorphine (Buprenex, 0.01 mg/kg, i.m.). If an animal developed partial or generalized seizures, it was given phenobarbital (2–6 mg/kg, i.m., until the seizures were controlled; up to 40 mg/kg in a 24 hr period).

Virus transport between neurons is time dependent (Zemanick et al., 1991; Strick and Card, 1992; Hoover and Strick, 1999; Middleton and Strick, 2001). Therefore, the number of hours that an animal survives after an injection determines how many synapses will be crossed. In the present study, animals were allowed to survive for 5–6 d after the virus injections. This time period permitted transneuronal transport to second-order but not third-order neurons (Strick and Card, 1992; Hoover and Strick, 1999; Middleton and Strick, 2001).

At the end of the survival period, each animal was deeply anesthetized (ketamine hydrochloride, 25 mg/kg, i.m.; pentobarbital sodium, 36–40 mg/kg, i.p.) and transcardially perfused using a three-step procedure (Rosene and Mesulam, 1978). The perfusates included 0.1 M PBS, 4% (w/v) paraformaldehyde in PBS, and 4% paraformaldehyde in PBS with 10% (v/v) glycerin. After the perfusion, the brain and cerebellum were photographed, stereotaxically blocked, removed from the cranium, and stored in buffered 4% paraformaldehyde with 20% glycerin (4°C) for 4–7 d.

Histology. Blocks of brain were frozen (Rosene et al., 1986) and serially sectioned in the coronal plane at a thickness of 50 μm. Every 10th section was counterstained with cresyl violet for cytoarchitectonic analysis [E. C. Gower in Mesulam (1982)]. To identify neurons labeled by virus transport, we processed free-floating tissue sections according to the avidin–biotin–peroxidase method (ABC; Vectastain; Vector Laboratories, Burlingame, CA) using a commercially available antibody to HSV1 (Dako, Carpinteria, CA; 1:2000 dilution). At least every other section from these animals was reacted. Sections were mounted onto gelatin-coated glass slides, air dried, and then coverslipped with either Artmount or DPX.

Analytic procedures. Approximately every other section was processed and examined for labeled neurons under bright-field, dark-field, and polarized illumination. Sections through the injection sites, frontal lobe, superior colliculus, hippocampus, and dentate nucleus were plotted using a computerized charting system (MD2; MN Datametrics, St. Paul, MN). This system uses optical encoders to sense *x–y* movements of the microscope stage and stores the coordinates of charted structures (e.g., section outlines, injection site zones, and labeled neurons). Digital images of selected structures were "captured" from the microscope using a video camera coupled to a high-resolution video processing board in a personal computer. Software written in the laboratory enabled us to generate high-resolution composites from multiple images.

The frequency of plotting varied according to the dimensions of the structure and ranged between 100 and 500 μm intervals. Sections through the superior colliculus were charted while wet and uncoverslipped to take advantage of the differential refractive index of myelin compared with neuron cell bodies. This technique allowed the layers of the superior colliculus to be clearly visualized in tissue that had not been subjected to traditional myelin stains, a process that is not compatible with immunostaining.

Determination of injection sites. Three concentric zones of labeling characterize virus injection sites (Strick and Card, 1992; Hoover and Strick, 1999). Zone I contains the needle track and the highest density of viral staining and pathology. In some instances, the tissue in this zone disintegrates during tissue processing. Zone II contains a dense accumulation of infected neurons and glia, as well as a high degree of background staining. Zone III contains large numbers of labeled neurons but little or no background staining. There is evidence that the actual zone of uptake for transneuronal transport of HSV1 is limited to zone I [for discussion of this issue, see Strick and Card (1992); Hoover and Strick (1999)].

The combination of subpial aspiration of the medial bank of the parietal sulcus and injection of HSV1 into the lateral bank caused significant tissue destruction in reacted sections containing the injection site. Therefore, to aid our determination of the spread of virus at the injection site, we plotted the distribution of first-order labeling in the IPL of the contralateral hemisphere and in the ipsilateral frontal lobe. We identified these regions of first-order labeling on the basis of the presence of large numbers of labeled and lysed neurons in the terminal stages of infection and intense background staining.

RESULTS

We made injections of HSV1 into the IPL of four *C. apella* monkeys. One animal (W06L) received a large injection that included LIP and portions of areas 7a and 7b. Each of the other

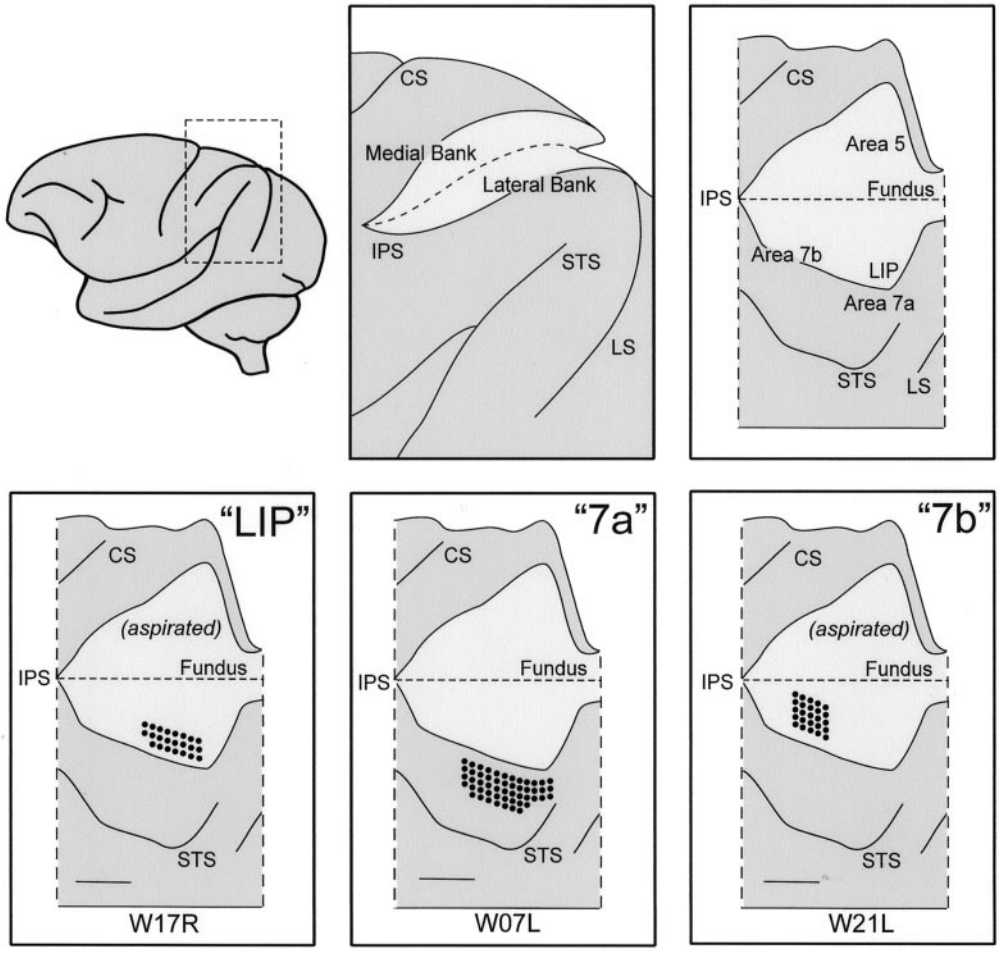

Figure 1. Schematic diagrams of injection sites. *Top left*, Lateral view of the hemisphere. *Top middle*, Enlarged view of the posterior parietal cortex (the region *boxed* in the *top left*). The intraparietal sulcus is opened in this diagram. *Top right*, Flattened map of the intraparietal sulcus. *Bottom row*, Flattened maps in the region of the intraparietal sulcus showing the targets for injection sites. Each *dot* represents the target for a single penetration of the injection syringe needle. *Bottom left*, Animal W17R, the *LIP* injection site. *Bottom middle*, Animal W07L, the *7a* injection site. *Bottom right*, Animal W21L, the *7b* injection site. All unfolded maps are oriented for display as the left hemisphere to facilitate comparison. Portions of the medial bank of the intraparietal sulcus were aspirated in animals W17R and W21L. Scale bars, 5.0 mm. *CS*, Central sulcus; *IPS*, intraparietal sulcus; *LS*, lunate sulcus; *STS*, superior temporal sulcus.

animals received more focused injections into either LIP (W17R), area 7a (W07L), or area 7b (W21L). We then examined second-order labeling at subcortical sites including the superior colliculus, hippocampus, cerebellum, globus pallidus, and substantia nigra. In the first section of our results we will describe the injection sites, in the second section we will briefly discuss thalamic labeling, and in the third section we will present the patterns of second-order labeling.

Characterization of injection sites

The injections of virus in W17R were placed entirely in the lateral (or caudal) bank of the intraparietal sulcus in LIP of the *Cebus* monkey (Tian and Lynch, 1996) (Fig. 1, *bottom left*). The injections in W07L were placed in area 7a on the cortical surface, caudal and lateral to LIP (Fig. 1, *bottom middle*). The injections in W21L were placed in the part of area 7b that is located rostrally in the lateral bank of the intraparietal sulcus (Fig. 1, *bottom right*). The injections in W06L were placed in the superficial, middle, and deep thirds of the lateral bank of the intraparietal sulcus (data not shown). The intent of the injections in W06L was to cover the full medial–lateral and rostrocaudal extent of LIP.

As noted in Materials and Methods, we observed significant tissue destruction at the sites of virus injection. To confirm the placement of injection sites, we examined the distribution of first-order labeling in the contralateral IPL. Callosal projections are known to interconnect complimentary regions of the IPL (Divac et al., 1977; Andersen et al., 1985; Neal, 1990; Lewis and Van Essen, 2000), and in W17R, W07L, and W21L, we found dense first-order labeling in the contralateral hemisphere at locations that mirrored the injection sites indicated in Figure 1. The injections in W06L resulted in first-order labeling not only in contralateral LIP but also in adjacent portions of area 7a and area 7b.

The functional subdivisions of the IPL are known to have unique patterns of connections with the frontal lobe (Andersen et al., 1985, 1990; Cavada and Goldman-Rakic, 1989b; Stanton et al., 1995; Lewis and Van Essen, 2000). Briefly, LIP is known to be interconnected with the FEF. In fact, this region of posterior parietal cortex was initially defined by this connection (Seltzer and Pandya, 1980; Barbas and Mesulam, 1981; Andersen et al., 1985). Area 7b is interconnected with the PMv (Cavada and Goldman-Rakic, 1989b; Kurata, 1991). Area 7a is interconnected with the supplementary eye field (SEF) and caudal portions of the cingulate gyrus (CGc) (Andersen et al., 1990), but not with the FEF or the PMv. To characterize the injection sites further, we examined four areas in the frontal lobe for first-order labeling: FEF, PMv, SEF, and CGc. We found massive first-order labeling in the "saccadic subregion" of the FEF only in W17R and in W06L. Dense first-order labeling in the PMv of the *Cebus* monkey (R. P. Dum and P. L. Strick, unpublished observations) was present only in W21L and in W06L. Dense first-order labeling was present in the SEF and CGc only in W07L and in W06L. On the basis of the labeling in the contralateral IPL and in the frontal lobe, we will refer to W17R as the "LIP" animal, W07L as the "7a" animal, and W21L as the "7b" animal. We will refer to W06L as the "Multi" animal, because the labeling in the contralateral

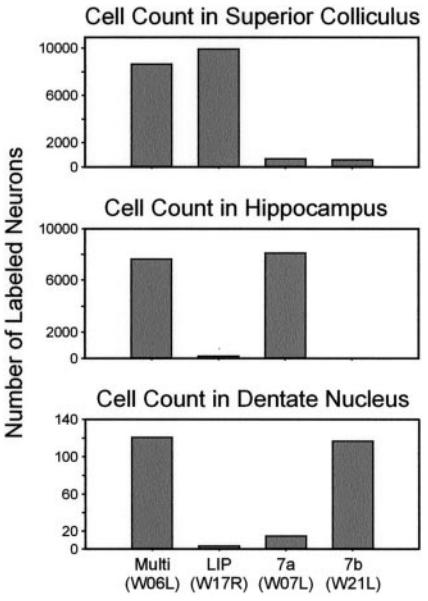

Figure 2. Quantification of second-order labeled neurons. The bar graphs depict the number of labeled neurons in each animal in the superior colliculus (*top*), hippocampus (*middle*), and dentate nucleus (*bottom*). Cell counts are normalized to the highest frequency of sampling (every 100 micrometers).

IPL and in the frontal lobe indicates that the injection site included LIP and portions of area 7a and area 7b. Thus, the Multi animal serves as a "second" case for each of the experiments with more focal injection sites.

Thalamic labeling

Injections of HSV1 into IPL led to dense labeling in thalamic nuclei known to be the origin of input to each cortical region (Kasdon and Jacobson, 1978; Asanuma et al., 1985; Schmahmann and Pandya, 1990; Hardy and Lynch, 1992; Baizer et al., 1993). Labeled neurons were found in other thalamic nuclei as well. This is not surprising because survival times were set to reveal second-order neurons. As a consequence, some of the labeled neurons in the thalamus represent second-order neurons labeled by retrograde transneuronal transport of virus via first-order neurons in cortical areas that innervate the injection site (Hoover and Strick, 1999).

Distribution of second-order labeling

We found second-order neurons, labeled by retrograde transneuronal transport of HSV1, at three major subcortical sites after virus injections into the IPL: the superior colliculus, the hippocampus, and the dentate nucleus of the cerebellum. The presence of second-order neurons at these subcortical sites depended on the portion of IPL injected (Fig. 2). Specifically, all injection sites that included LIP resulted in second-order neurons in the superior colliculus. Injection sites that included area 7a labeled neurons in the hippocampus, whereas injections that included area 7b labeled neurons in the dentate nucleus of the cerebellum.

It is important to note that the three subcortical sites where we found labeled neurons do not project monosynaptically to the cortical areas under study (Divac et al., 1977; Morecraft et al., 1993). Furthermore, the survival time we used (5–6 d) has been shown in previous studies to label second-order but not third-order neurons (Zemanick et al., 1991; Strick and Card, 1992; Hoover and Strick, 1999; Middleton and Strick, 2001). Thus, the labeled neurons in the superior colliculus, hippocampus, and dentate nucleus are termed "second-order" because they have disynaptic connections with the regions injected with HSV1 and are labeled via retrograde transneuronal transport of virus.

Superior colliculus

Most of the second-order neurons labeled in the superior colliculus after virus injections into LIP were found ipsilateral to the injection site. However, unilateral injections of virus also resulted in a small number of labeled neurons in the contralateral superior colliculus. In the LIP animal, almost all of the second-order neurons were found ipsilaterally in the caudal half of the colliculus. Similarly, most of the second-order neurons were located in the caudal half of the colliculus in the Multi animal; however a small portion of the total sample (20%) was found in the rostral half of the colliculus (Fig. 3, *left*). On the basis of this differential distribution, a topography may exist in the projection from the colliculus to LIP, although further experiments are necessary to explore this possibility.

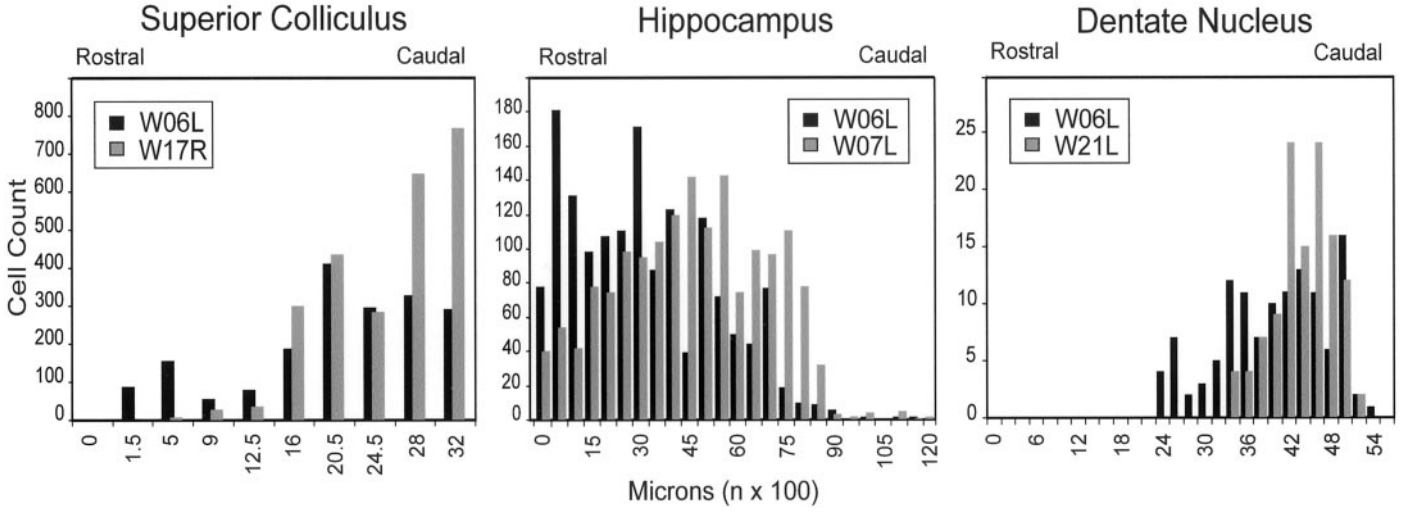

Figure 3. Distribution of second-order labeled neurons. The histograms show the rostrocaudal distribution of labeling in the superior colliculus for W06L (Multi) versus W17R (LIP) (*left*), in the hippocampus for W06L (Multi) versus W07L (7a) (*middle*), and in the dentate nucleus for W06L (Multi) versus W21L (7b) (*right*).

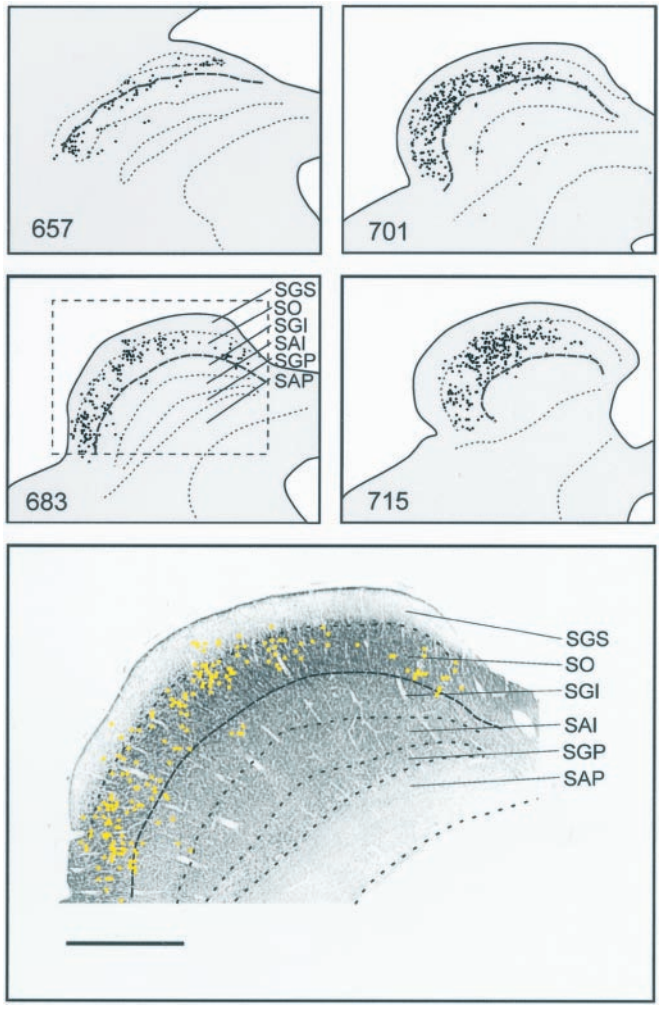

Figure 4. Second-order labeling in the superior colliculus after injections including LIP. *Top four panels*, Plots of sections (section numbers in *bottom left corner*) through the superior colliculus of W06L. Each *black dot* indicates one labeled neuron, and *dotted lines* indicate the borders between layers. A *darker dashed line* indicates the border between superficial and intermediate layers of the superior colliculus. *Bottom panel*, The location of labeled cells (in *yellow*) superimposed on a photomicrograph of the *boxed region* in the *683 panel*. Scale bar, 1.0 mm. *SAI*, Stratum album intermedium; *SAP*, stratum album profundum; *SGI*, stratum griseum intermedium; *SGP*, stratum griseum profundum; *SGS*, stratum griseum superficiale; *SO*, stratum opticum.

The laminar distribution of second-order neurons varied with their rostrocaudal location (Fig. 4). Second-order neurons in the caudal half of the colliculus were located predominantly (91%) in the superficial or visual layers (stratum griseum superficiale and stratum opticum). In contrast, neurons labeled in the rostral half of the colliculus were located in both the superficial (59%) and intermediate layers (stratum griseum intermediale; 41%). A very small number of the second-order neurons also were located in the deep layers of the colliculus (e.g., 27/1901 labeled neurons in the Multi animal).

Hippocampus

Second-order neurons labeled in the hippocampus after virus injections into area 7a were found primarily ipsilateral to the injection site, although a small number were found contralaterally. The labeled neurons were found in the pyramidal cell layer of the CA1 region. The region of CA1 that contained labeled neurons occupied the central third in the transverse plane and primarily the rostral three-quarters in the longitudinal axis (Fig. 5). The population of labeled neurons in the area 7a animal was centered slightly caudal to that of the Multi animal (Fig. 3, *middle*).

Deep cerebellar nuclei

Second-order neurons labeled in the deep cerebellar nuclei after virus injections into area 7b were found in the dentate nucleus contralateral to the injection site (Fig. 6). Labeled neurons were located throughout the caudal half of the dentate. The greatest density of these neurons was found ventrally in the caudal third of the nucleus (Figs. 3, *right,* 6). The population of labeled neurons in the Multi animal extended more rostrally in the dentate than did that of the area 7b animal (Fig. 3). The dentate neurons labeled from virus injections into area 7b had characteristics that were typical of "projection" neurons in the deep cerebellar nuclei.

An additional dense patch of second-order neurons was labeled in a ventral and caudal site within the PIP of the Multi animal. This region of PIP contains neurons with activity related to eye movements (van Kan et al., 1993; Zhang and Gamlin, 1998). Labeled neurons were not found at this site in the area 7b animal or in any of the other animals of this study. Further experiments are necessary to determine whether a subregion of LIP, area 7b, or an adjacent region of the IPL such as the ventral intraparietal area is the source of this labeling.

DISCUSSION

We found that IPL is the target of disynaptic output from three subcortical sites: the superior colliculus, the hippocampus, and the cerebellum. In fact, each subcortical region innervates a different area of the IPL (Fig. 7). LIP receives input from visual layers of the superior colliculus, area 7a receives input from the CA1 region of the hippocampus, and area 7b receives input from the dentate nucleus. This discussion will focus on the functional implications of these segregated inputs.

Superior colliculus to LIP

It is known from experiments with conventional tracers that the superficial, "visual" layers of the superior colliculus project to the lateral pulvinar nucleus in the thalamus (Harting et al., 1980; Benevento and Standage, 1983). Similarly, a dorsal portion of the lateral pulvinar projects to LIP (Asanuma et al., 1985; Hardy and Lynch, 1992; Baizer et al., 1993). Our results suggest that neurons in the lateral pulvinar mediate a projection from the superficial layers of the superior colliculus to LIP. Neurons in these layers have visual receptive fields that are retinotopically organized (Lund, 1972; Sparks, 1986). Thus, it is likely that input from the colliculus contributes to the visual responses of LIP neurons (Blatt et al., 1990; Barash et al., 1991a,b).

We found that most of the second-order neurons labeled after LIP injections were located in the caudal portion of the colliculus where the peripheral visual field is represented (Cynader and Berman, 1972; Goldberg and Wurtz, 1972a). However, the larger injection site in LIP labeled some second-order neurons in the rostral portion of the colliculus where the fovea is represented. These observations suggest that the projection from the superior colliculus to LIP is topographically organized. Furthermore, the rough topographic organization of visual receptive fields seen in LIP (Blatt et al., 1990) may be partly a consequence of collicular input. In this respect, it is interesting that approximately one-

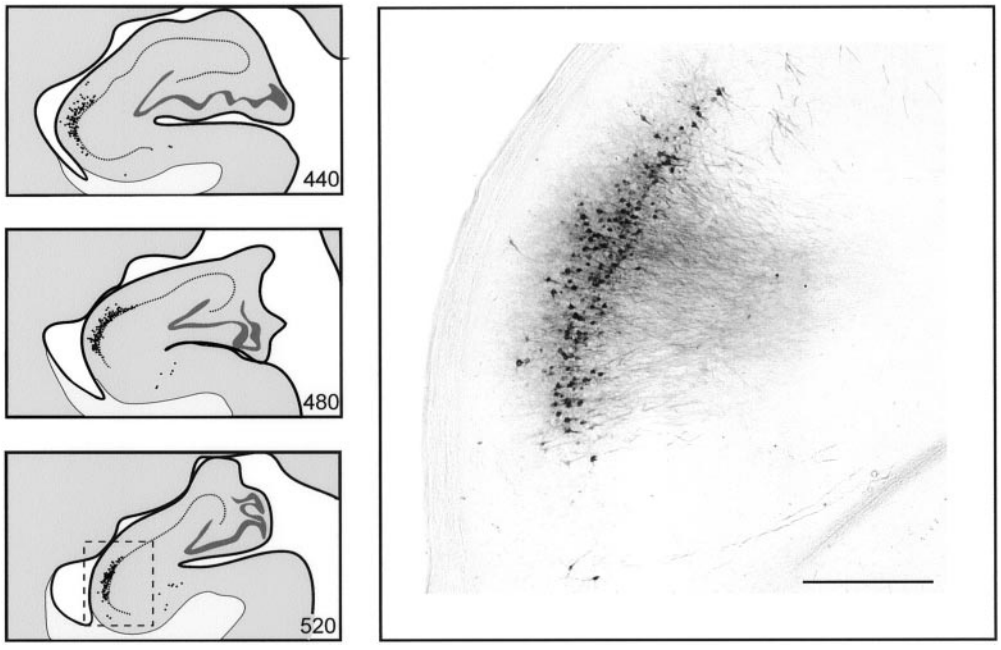

Figure 5. Second-order labeling in the hippocampus after injections including area 7a. *Left*, Plots of sections (section numbers in *bottom right corner*) through the hippocampus of W07L. Each *black dot* indicates one labeled neuron. *Right*, A photomicrograph of the region *outlined* in the *bottom left* section. Scale bar, 500 μm.

quarter of the corticotectal neurons in LIP reported by Paré and Wurtz (1997) respond to foveal stimuli. Similarly, a comparable percentage of tectal input to LIP appears to originate from the rostral (foveal) portion of the colliculus.

As noted above, our results demonstrate that the superficial layers provide the majority of the collicular input to LIP. In contrast, the intermediate layers receive the majority of the output from LIP (Lynch et al., 1985). Thus, there is a clear "open loop" bias in the flow of information. This pattern of information flow is evident in the physiological properties of the neurons in the regions that form this circuit. Certain properties, such as presaccadic enhancement of visual responses, are present in both the superficial layers of the colliculus and LIP, but not in the intermediate layers of the colliculus (Goldberg and Wurtz, 1972b; Wurtz and Mohler, 1976; Goldberg et al., 1990; Colby et al., 1993). Likewise, sustained delay period activity related to an upcoming eye movement is present in both LIP and the intermediate layers of the colliculus, but not in the superficial layers (Mazzoni et al., 1996; Paré and Wurtz, 1997; Snyder et al., 1997). Thus, our results are consistent with the classical view that the superficial layers of the colliculus are a source of disynaptic visual input to LIP and that LIP sends signals related to oculomotor function back to the intermediate layers (Lynch, 1980, 1992; Lynch et al., 1985; Tian and Lynch, 1996).

In a previous study using similar methods (Lynch et al., 1994), we found that a larger proportion of the collicular input to FEF originates from the intermediate layers where activity is predominantly related to the generation of saccades (Sparks, 1986). Thus, it is likely that the collicular input to FEF is biased toward oculomotor function, whereas that to LIP is biased toward visual processing. On the other hand, a small percentage (<15%) of the cells labeled after LIP injections were found in intermediate layers. Consequently, collicular input to LIP may contribute to oculomotor function as well.

Hippocampus to area 7a

Perhaps our most surprising finding is the demonstration that area 7a in the posterior parietal cortex receives a strong disynaptic input from the CA1 region of the hippocampus. The pyramidal cells labeled in our study were found primarily in the central strip of the CA1 region, in the rostral three-quarters of the hippocampus. The central portion of CA1 projects to area TF of the parahippocampal gyrus (Blatt and Rosene, 1998), and area TF is reciprocally connected with area 7a (Andersen et al., 1990). Thus, area TF is likely to mediate the projection from CA1 to area 7a.

Previous studies have shown that CA1 receives direct projections from area 7a (and area 7b) (Cavada and Goldman-Rakic, 1989a; Rockland and Van Hoesen, 1999). There is considerable evidence that CA1 participates in a spatial memory system useful for navigation (Rolls et al., 1997, 1998; Rolls, 1999). Similarly, area 7a has been implicated in spatial processing. For example, area 7a neurons display visual responses that are modulated by both head and body position (Snyder et al., 1998). In addition, the responses of some area 7a neurons show an interactive dependence on both speed and direction of optic flow (Phinney and Siegel, 2000). This property might contribute to the perception of self-motion and heading during navigation. Thus, input from area 7a to CA1 could influence some of the spatial properties of CA1 neurons.

Our results emphasize a different perspective, namely, that CA1 may contribute to the construction of responses in area 7a. In fact, the CA1 region that sends a disynaptic projection to area 7a is considerably more extensive than is the CA1 region that receives from area 7a. The portion of CA1 that receives direct input from area 7a is located in a small area that is posterior (along the longitudinal axis) and distal (along the transverse axis) to the large CA1 region that projects to area 7a. Thus, although the hippocampus receives from area 7a and projects to area 7a, this pathway does not appear to be a simple "closed loop" circuit. Furthermore, the most significant direction of information flow may be from CA1 to area 7a rather than the reverse.

Human imaging and lesion studies support the concept that a functional linkage exists between the hippocampus and the posterior parietal cortex (Kesner et al., 1991; Berthoz, 1997). Tasks involving spatial navigation result in activation of portions of both the posterior parietal cortex and the hippocampus (Maguire et al.,

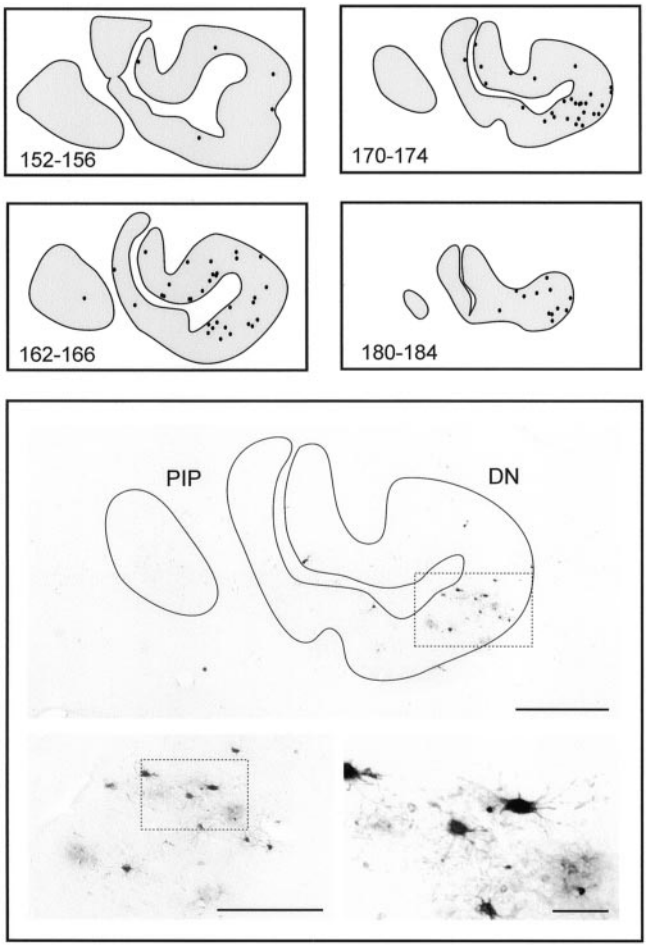

Figure 6. Second-order labeling in the dentate nucleus after injections including area 7b. *Top four panels*, Plots of sections (section numbers in *bottom left corner*) through the dentate nucleus of W21L. Each *black dot* indicates one labeled neuron. Labeled cells from three consecutive sections spaced 100 μm apart are superimposed on each plot. *Bottom panel*, Labeled neurons in the dentate of W21L. These neurons were found on section 172. The region enlarged on the *bottom left* is indicated by the *box* on the *top right*. The region enlarged on the *bottom right* is indicated by the *box* on the *bottom left*. Scale bars (*bottom panel*): *top*, 1000 μm; *bottom left*, 500 μm; *bottom right*, 100 μm. *DN*, Dentate nucleus; *PIP*, posterior interpositus.

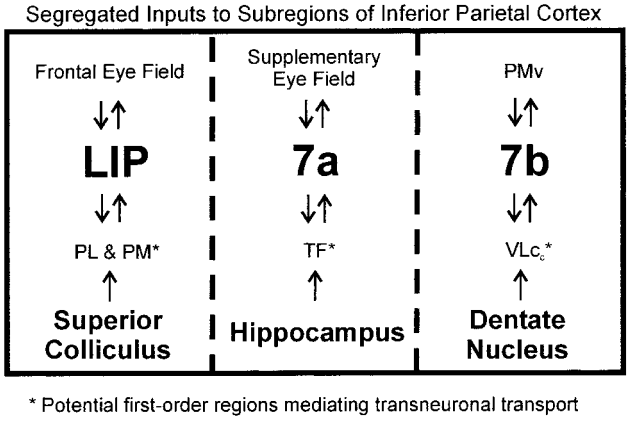

Figure 7. Subcortical inputs to posterior parietal subregions. Each subregion of the posterior parietal cortex that we examined receives input from a different subcortical site. The potential first-order regions that mediate these connections are indicated by *asterisks*. The diagram also indicates the unique "motor" areas in the frontal lobe that are interconnected with each parietal subregion. The *double arrows* indicate reciprocal connections. *PL*, Lateral pulvinar nucleus; *PM*, medial pulvinar nucleus; *VLc*, ventral lateral nucleus, pars caudalis.

1998; Gron et al., 2000). Similarly, damage to either the hippocampus or posterior parietal cortex leads to difficulty in route finding (Barrash, 1998; Barrash et al., 2000). Our results provide an anatomical substrate for linking these two brain regions into a parietohippocampal network for spatial navigation. We suggest that the disynaptic projection from CA1 to area 7a should be viewed as the efferent limb of this circuit. Such a pathway would allow the memory functions of the hippocampus to influence the spatial processing in area 7a.

Dentate nucleus to area 7b

The cerebellum is the third subcortical site that we identified as a source of second-order input to IPL. This pathway originates from the dentate nucleus and terminates in a portion of area 7b. It is likely that the dentate projection to area 7b is mediated primarily by thalamocortical projections from the caudal portion of VLc. Caudal VLc and some adjacent subdivisions of the ventrolateral thalamus receive dentate input, and these same thalamic subdivisions project to regions of the IPL in or near area 7b (see also Sasaki et al., 1976; Kasdon and Jacobson, 1978; Miyata and Sasaki, 1983; Asanuma et al., 1985; Schmahmann and Pandya, 1990).

In previous studies, we found that a number of motor and nonmotor regions in the frontal lobe are the target of dentate output. Neurons that project to each of these cortical areas are clustered in spatially separate regions of the dentate and form distinct "output channels" (Middleton and Strick, 1994, 1998, 2001). In the present study, the dentate neurons that target area 7b are predominantly located in a ventral region within the caudal third of the nucleus. This region is posterior to the dentate output channel that innervates M1, and it is nested between the channels that project to the hand region of PMv and the saccadic subregion of the FEF (Strick et al., 1993; Lynch et al., 1994; Hoover and Strick, 1999). Thus, the present results suggest that the dentate contains a distinct output channel that targets a portion of the posterior parietal cortex.

We found that area 7a and LIP receive scant cerebellar input. This suggests that the cerebellum directly influences limited portions of the IPL. However, we have examined the inputs to a relatively small portion of the posterior parietal cortex. Previous electrophysiological studies in the monkey have provided evidence of a projection from the fastigial nucleus to a portion of parietal area 5 (Sasaki et al., 1976; Miyata and Sasaki, 1983). Similarly, in the cat there appears to be a projection from the dentate and interpositus to areas 5 and 7 (Wannier et al., 1992; Kakei et al., 1995). Thus, it is likely that the cerebellum gains access to multiple areas of the posterior parietal cortex, and the complete set of parietal areas that are the target of cerebellar output remains to be determined.

Classically, cerebellar function was thought to be limited to the domain of motor control. A number of recent observations have led to some alteration in this point of view (Leiner et al., 1986, 1993; Botez et al., 1989; Ivry and Keele, 1989; Schmahmann, 1991, 1997a,b; Akshoomoff and Courchesne, 1992; Fiez et al., 1992; Schmahmann and Sherman, 1998). For example, Middleton and Strick (1994, 1998, 2001) have shown that there are output channels in the dentate that innervate regions of prefrontal cortex. Cerebellar lesions in humans cause cognitive deficits (Graf-

man et al., 1992; Drepper et al., 1999), and cognitive tasks lead to functional activation of cerebellar structures (Petersen et al., 1988; Kim et al., 1994; Raichle et al., 1994; Fiez et al., 1996; Gao et al., 1996; Cabeza and Nyberg, 2000). Our finding that the dentate also contains an output channel that disynaptically innervates a subregion of IPL suggests that concepts about cerebellar function should be expanded further to include a potential contribution to sensory processing (see also Gao et al., 1996; Ivry, 2000).

At this point, we can only speculate on what the cerebellum might contribute to the function of posterior parietal cortex. However, some important clues may come from the results of recent studies on the neural basis of prism adaptation. When vision is displaced by prisms, systematic errors in reaching movements occur. In addition, the prisms induce a sensory mismatch between the visual and proprioceptive representations of the limb (see Harris, 1965; Welch, 1986). As a consequence, the process of prism adaptation involves at least two components, a motor component involving the correction of errors in motor output and a perceptual component involving a recalibration of sensory representations. The cerebellum has long been thought to participate in the motor component of this process (Marr, 1969; Oscarsson, 1969; Ito, 1993; Thach, 1998; Baizer et al., 1999). Cerebellar projections to motor areas in the frontal lobe may represent part of the neural substrate for adapting motor performance. Likewise, the posterior parietal cortex has been implicated in the perceptual recalibration associated with prism adaptation (Clower et al., 1996; Rossetti et al., 1998). We suggest that the cerebellar projection to posterior parietal cortex may provide signals that contribute to (or initiate) the sensory recalibration that occurs during the adaptive process.

REFERENCES

Akshoomoff NA, Courchesne E (1992) A new role for the cerebellum in cognitive function. Behav Neurosci 106:731–738.

Andersen RA (1989) Visual and eye movement functions of the posterior parietal cortex. Annu Rev Neurosci 12:377–403.

Andersen RA, Asanuma C, Cowan WM (1985) Callosal and prefrontal associational projecting cell populations in area 7A of the macaque monkey: a study using retrogradely transported fluorescent dyes. J Comp Neurol 232:443–455.

Andersen RA, Asanuma C, Essick GK, Siegel RM (1990) Corticocortical connections of anatomically and physiologically defined subdivisions within the inferior parietal lobule. J Comp Neurol 296:65–113.

Asanuma C, Andersen RA, Cowan WM (1985) The thalamic relations of the caudal inferior parietal lobule and the lateral prefrontal cortex in monkeys: divergent cortical projections from cell clusters in the medial pulvinar nucleus. J Comp Neurol 241:357–381.

Baizer JS, Desimone R, Ungerleider LG (1993) Comparison of subcortical connections of inferior temporal and posterior parietal cortex in monkeys. Vis Neurosci 10:59–72.

Baizer JS, Kralj-Hans I, Glickstein M (1999) Cerebellar lesions and prism adaptation in macaque monkeys. J Neurophysiol 81:1960–1965.

Barash S, Bracewell RM, Fogassi L, Gnadt JW, Andersen RA (1991a) Saccade-related activity in the lateral intraparietal area. I. Temporal properties; comparison with area 7a. J Neurophysiol 66:1095–1108.

Barash S, Bracewell RM, Fogassi L, Gnadt JW, Andersen RA (1991b) Saccade-related activity in the lateral intraparietal area. II. Spatial properties. J Neurophysiol 66:1109–1124.

Barbas H, Mesulam MM (1981) Organization of afferent input to subdivisions of area 8 in the rhesus monkey. J Comp Neurol 200:407–431.

Barrash J (1998) A historical review of topographical disorientation and its neuroanatomical correlates. J Clin Exp Neuropsychol 20:807–827.

Barrash J, Damasio H, Adolphs R, Tranel D (2000) The neuroanatomical correlates of route learning impairment. Neuropsychologia 38:820–836.

Benevento LA, Standage GP (1983) The organization of projections of the retinorecipient and nonretinorecipient nuclei of the pretectal complex and layers of the superior colliculus to the lateral pulvinar and medial pulvinar in the macaque monkey. J Comp Neurol 217:307–336.

Berthoz A (1997) Parietal and hippocampal contribution to topokinetic and topographic memory. Philos Trans R Soc Lond B Biol Sci 352:1437–1448.

Blatt GJ, Rosene DL (1998) Organization of direct hippocampal efferent projections to the cerebral cortex of the rhesus monkey: projections from CA1, prosubiculum, and subiculum to the temporal lobe. J Comp Neurol 392:92–114.

Blatt GJ, Andersen RA, Stoner GR (1990) Visual receptive field organization and cortico-cortical connections of the lateral interparietal area (area LIP) in the macaque. J Comp Neurol 299:421–445.

Botez MI, Botez T, Elie R, Attig E (1989) Role of the cerebellum in complex human behavior. Ital J Neurol Sci 10:291–300.

Cabeza R, Nyberg L (2000) Imaging cognition. II. An empirical review of 275 PET and fMRI studies. J Cognit Neurosci 12:1–47.

Cavada C, Goldman-Rakic PS (1989a) Posterior parietal cortex in rhesus monkey. I. Parcellation of areas based on distinctive limbic and sensory corticocortical connections. J Comp Neurol 287:393–421.

Cavada C, Goldman-Rakic PS (1989b) Posterior parietal cortex in rhesus monkey. II. Evidence for segregated corticocortical networks linking sensory and limbic areas with frontal lobe. J Comp Neurol 287:422–445.

Cavada C, Goldman-Rakic PS (1991) Topographic segregation of corticostriatal projections from posterior parietal subdivisions in the macaque monkey. Neuroscience 42:683–696.

Clower DM, Hoffman JM, Votaw JR, Faber TL, Woods RP, Alexander GE (1996) Role of posterior parietal cortex in the recalibration of visually guided reaching. Nature 383:618–621.

Colby CL, Goldberg ME (1999) Space and attention in parietal cortex. Annu Rev Neurosci 22:319–349.

Colby CL, Duhamel JR, Goldberg ME (1993) The analysis of visual space by the lateral intraparietal area of the monkey: the role of extraretinal signals. Prog Brain Res 95:307–316.

Colby CL, Duhamel JR, Goldberg ME (1996) Visual, presaccadic, and cognitive activation of single neurons in monkey lateral intraparietal area. J Neurophysiol 76:2841–2852.

Cynader M, Berman N (1972) Receptive-field organization of monkey superior colliculus. J Neurophysiol 35:187–201.

Divac I, LaVail JH, Rakic P, Winston KR (1977) Heterogeneous afferents to the inferior parietal lobule of the rhesus monkey revealed by the retrograde transport method. Brain Res 123:197–207.

Drepper J, Timmann D, Kolb FP, Diener HC (1999) Non-motor associative learning in patients with isolated degenerative cerebellar disease. Brain 122:87–97.

Fiez JA, Petersen SE, Cheney MK, Raichle ME (1992) Impaired nonmotor learning and error detection associated with cerebellar damage. Brain 115:155–178.

Fiez JA, Raife EA, Balota DA, Schwarz JP, Raichle ME, Petersen SE (1996) A positron emission tomography study of the short-term maintenance of verbal information. J Neurosci 16:808–822.

Gao JH, Parsons LM, Bower JM, Xiong J, Li J, Fox PT (1996) Cerebellum implicated in sensory acquisition and discrimination rather than motor control. Science 272:545–547.

Goldberg ME, Wurtz RH (1972a) Activity of superior colliculus in behaving monkey. I. Visual receptive fields of single neurons. J Neurophysiol 35:542–559.

Goldberg ME, Wurtz RH (1972b) Activity of superior colliculus in behaving monkey. II. Effect of attention on neuronal responses. J Neurophysiol 35:560–574.

Goldberg ME, Colby CL, Duhamel JR (1990) Representation of visuomotor space in the parietal lobe of the monkey. Cold Spring Harb Symp Quant Biol 55:729–739.

Grafman J, Litvan I, Massaquoi S, Stewart M, Sirigu A, Hallett M (1992) Cognitive planning deficit in patients with cerebellar atrophy. Neurology 42:1493–1496.

Gron G, Wunderlich AP, Spitzer M, Tomczak R, Riepe MW (2000) Brain activation during human navigation: gender-different neural networks as substrate of performance. Nat Neurosci 3:404–408.

Hardy SG, Lynch JC (1992) The spatial distribution of pulvinar neurons that project to two subregions of the inferior parietal lobule in the macaque. Cereb Cortex 2:217–230.

Harris CS (1965) Perceptual adaptation to inverted, reversed and displaced vision. Psychol Rev 72:419–444.

Harting JK, Huerta MF, Frankfurter AJ, Strominger NL, Royce GJ (1980) Ascending pathways from the monkey superior colliculus: an autoradiographic analysis. J Comp Neurol 192:853–882.

Hoover JE, Strick PL (1999) The organization of cerebellar and basal ganglia outputs to primary motor cortex as revealed by retrograde transneuronal transport of herpes simplex virus type 1. J Neurosci 19:1446–1463.

Hyvarinen J (1981) Regional distribution of functions in parietal association area 7 of the monkey. Brain Res 206:287–303.

Ito M (1993) Synaptic plasticity in the cerebellar cortex and its role in motor learning. Can J Neurol Sci 20 [Suppl 3]:S70–S74.

Ivry R (2000) Exploring the role of the cerebellum in sensory anticipation and timing: commentary on Tesche and Karhu. Hum Brain Mapp 9:115–118.

Ivry RB, Keele SW (1989) Timing functions of the cerebellum. J Cognit Neurosci 1:136–152.

Kakei S, Yagi J, Wannier T, Na J, Shinoda Y (1995) Cerebellar and

cerebral inputs to corticocortical and corticofugal neurons in areas 5 and 7 in the cat. J Neurophysiol 74:400–412.
Kasdon DL, Jacobson S (1978) The thalamic afferents to the inferior parietal lobule of the rhesus monkey. J Comp Neurol 177:685–706.
Kesner RP, Farnsworth G, Kametani H (1991) Role of parietal cortex and hippocampus in representing spatial information. Cereb Cortex 1:367–373.
Kim S-G, Ugurbil K, Strick PL (1994) Activation of a cerebellar output nucleus during cognitive processing. Science 265:949–951.
Kurata K (1991) Corticocortical inputs to the dorsal and ventral aspects of the premotor cortex of macaque monkeys. Neurosci Res 12:263–280.
Leiner HC, Leiner AL, Dow RS (1986) Does the cerebellum contribute to mental skills? Behav Neurosci 100:443–454.
Leiner HC, Leiner AL, Dow RS (1993) Cognitive and language functions of the human cerebellum. Trends Neurosci 16:444–447.
Lewis JW, Van Essen DC (2000) Corticocortical connections of visual sensorimotor and multimodal processing areas in the parietal lobe of the macaque monkey. J Comp Neurol 428:112–137.
Lund RD (1972) Synaptic patterns in the superficial layers of the superior colliculus of the monkey, *Macaca mulatta*. Exp Brain Res 15:194–211.
Lynch JC (1980) The functional organization of posterior parietal association cortex. Behav Brain Sci 3:485–534.
Lynch JC (1992) Saccade initiation and latency deficits after combined lesions of the frontal and posterior eye fields in monkeys. J Neurophysiol 68:1913–1916.
Lynch JC, Mountcastle VB, Talbot WH, Yin TCT (1977) Parietal lobe mechanisms for directed visual attention. J Neurophysiol 45:362–389.
Lynch JC, Graybiel AM, Lobeck LJ (1985) The differential projection of two cytoarchitectonic subregions of the inferior parietal lobule of macaque upon the deep layers of the superior colliculus. J Comp Neurol 235:241–254.
Lynch JC, Hoover JE, Strick PL (1994) Input to the primate frontal eye field from the substantia nigra, superior colliculus, and dentate nucleus demonstrated by transneuronal transport. Exp Brain Res 100:181–186.
Maguire EA, Burgess N, Donnett JG, Frackowiak RS, Frith CD, O'Keefe J (1998) Knowing where and getting there: a human navigation network. Science 280:921–924.
Marr D (1969) A theory of cerebellar cortex. J Physiol (Lond) 202:437–470.
May JG, Andersen RA (1986) Different patterns of corticopontine projections from separate cortical fields within the inferior parietal lobule and dorsal prelunate gyrus of the macaque. Exp Brain Res 63:265–278.
Mazzoni P, Bracewell RM, Barash S, Andersen RA (1996) Motor intention activity in the macaque's lateral intraparietal area. I. Dissociation of motor plan from sensory memory. J Neurophysiol 76:1439–1456.
Mesulam MM (1982) Tracing neuronal connections with horseradish peroxidase. New York: Wiley.
Middleton FA, Strick PL (1994) Anatomical evidence for cerebellar and basal ganglia involvement in higher cognitive function. Science 266:458–461.
Middleton FA, Strick PL (1998) The cerebellum: an overview. Trends Neurosci 21:367–369.
Middleton FA, Strick PL (2001) Cerebellar projections to the prefrontal cortex of the primate. J Neurosci 21:700–712.
Miyata M, Sasaki K (1983) HRP studies on thalamocortical neurons related to the cerebellocerebral projection in the monkey. Brain Res 274:213–224.
Morecraft RJ, Geula C, Mesulam MM (1993) Architecture of connectivity within a cingulo-fronto-parietal neurocognitive network for directed attention. Arch Neurol 50:279–284.
Murata A, Gallese V, Kaseda M, Sakata H (1996) Parietal neurons related to memory-guided hand manipulation. J Neurophysiol 75:2180–2186.
Neal JW (1990) The callosal connections of area 7b, PF in the monkey. Brain Res 514:159–162.
Oscarsson O (1969) Termination and functional organization of the dorsal spino-olivocerebellar path. J Physiol (Lond) 200:129–149.
Pandya DN, Seltzer B (1982) Intrinsic connections and architectonics of posterior parietal cortex in the rhesus monkey. J Comp Neurol 204:196–210.
Paré M, Wurtz RH (1997) Monkey posterior parietal cortex neurons antidromically activated from superior colliculus. J Neurophysiol 78:3493–3497.
Petersen SE, Fox PT, Posner MI, Mintun M, Raichle ME (1988) Positron emission tomographic studies of the cortical anatomy of single-word processing. Nature 331:585–589.
Phinney RE, Siegel RM (2000) Speed selectivity for optic flow in area 7a of the behaving macaque. Cereb Cortex 10:413–421.
Raichle ME, Fiez JA, Videen TO, MacLeod AM, Pardo JV, Fox PT, Petersen SE (1994) Practice-related changes in human brain functional anatomy during nonmotor learning. Cereb Cortex 4:8–26.
Rockland KS, Van Hoesen GW (1999) Some temporal and parietal cortical connections converge in CA1 of the primate hippocampus. Cereb Cortex 9:232–237.
Rolls ET (1999) Spatial view cells and the representation of place in the primate hippocampus. Hippocampus 9:467–480.
Rolls ET, Robertson RG, Georges-Francois P (1997) Spatial view cells in the primate hippocampus. Eur J Neurosci 9:1789–1794.
Rolls ET, Treves A, Robertson RG, Georges-Francois P, Panzeri S (1998) Information about spatial view in an ensemble of primate hippocampal cells. J Neurophysiol 79:1797–1813.
Rosene DL, Mesulam MM (1978) Fixation variables in horseradish peroxidase neurohistochemistry. I. The effect of fixation time and perfusion procedures upon enzyme activity. J Histochem Cytochem 26:28–39.
Rosene DL, Roy NJ, Davis BJ (1986) A cryoprotection method that facilitates cutting frozen sections of whole monkey brains for histological and histochemical processing without freezing artifact. J Histochem Cytochem 34:1301–1315.
Rossetti Y, Rode G, Pisella L, Farne A, Li L, Boisson D, Perenin MT (1998) Prism adaptation to a rightward optical deviation rehabilitates left hemispatial neglect. Nature 395:166–169.
Sakata H, Taira M, Murata A, Mine S (1995) Neural mechanisms of visual guidance of hand action in the parietal cortex of the monkey. Cereb Cortex 5:429–438.
Sasaki K, Kawaguchi S, Oka H, Sakai M, Mizuno N (1976) Electrophysiological studies on the cerebellocerebral projections in monkeys. Exp Brain Res 24:495–507.
Schmahmann JD (1991) An emerging concept. The cerebellar contribution to higher function. Arch Neurol 48:1178–1187.
Schmahmann JD (1997a) Rediscovery of an early concept. Int Rev Neurobiol 41:3–27.
Schmahmann JD, ed (1997b) The cerebellum and cognition. San Diego: Academic.
Schmahmann JD, Pandya DN (1990) Anatomical investigation of projections from thalamus to posterior parietal cortex in the rhesus monkey: a WGA-HRP and fluorescent tracer study. J Comp Neurol 295:299–326.
Schmahmann JD, Sherman JC (1998) The cerebellar cognitive affective syndrome. Brain 121:561–579.
Seltzer B, Pandya DN (1980) Converging visual and somatic sensory cortical input to the interparietal sulcus of the rhesus monkey. Brain Res 192:339–351.
Snyder LH, Batista AP, Andersen RA (1997) Coding of intention in the posterior parietal cortex. Nature 386:167–170.
Snyder LH, Grieve KL, Brotchie P, Andersen RA (1998) Separate body- and world-referenced representations of visual space in parietal cortex. Nature 394:887–891.
Sparks DL (1986) Translation of sensory signals into commands for control of saccadic eye movements: role of the primate superior colliculus. Physiol Rev 66:118–171.
Stanton GB, Bruce CJ, Goldberg ME (1995) Topography of projections to posterior cortical areas from the macaque frontal eye fields. J Comp Neurol 353:291–305.
Strick PL, Card JP (1992) Transneuronal mapping of neural circuits with alpha herpesviruses. In: Experimental neuroanatomy: a practical approach (Bolam JP, ed), pp 81–101. Oxford: Oxford UP.
Strick PL, Hoover JE, Mushiake H (1993) Evidence for "output channels" in the basal ganglia and cerebellum. In: Role of the cerebellum and basal ganglia in voluntary movement (Mano N, Hamada I, DeLong MR, eds), pp 171–180. Amsterdam: Elsevier.
Thach WT (1998) A role for the cerebellum in learning movement coordination. Neurobiol Learn Mem 70:177–188.
Tian J-R, Lynch JC (1996) Cortico-cortical input to the smooth and saccadic eye movement subregions in the frontal eye field in *Cebus* monkeys. J Neurophysiol 76:2754–2771.
van Kan PL, Houk JC, Gibson AR (1993) Output organization of intermediate cerebellum of the monkey. J Neurophysiol 69:57–73.
Wannier T, Kakei S, Shinoda Y (1992) Two modes of cerebellar input to the parietal cortex in the cat. Exp Brain Res 90:241–252.
Welch RB (1986) Adaptation of space perception. In: Handbook of perception and human performance, sensory processes and perception (Boff KR, Kaufman L, Thomas JP, eds), pp 1:24.1–1:24.45. New York: Wiley.
West RA, Lynch JC, Strick PL (1998) Superior colliculus inputs to the lateral intraparietal area (LIP) in the monkey. Soc Neurosci Abstr 24:418.
West RA, Clower DM, Lynch JC, Strick PL (1999) The inferior parietal lobule is the target of output from the superior colliculus, cerebellum, and hippocampus. Soc Neurosci Abstr 25:1402.
Wurtz RH, Mohler CW (1976) Organization of monkey superior colliculus: enhanced visual response of superficial layer cells. J Neurophysiol 39:745–765.
Zemanick MC, Strick PL, Dix RD (1991) Direction of transneuronal transport of herpes simplex virus 1 in the primate motor system is strain-dependent. Proc Natl Acad Sci USA 88:8048–8051.
Zhang H, Gamlin PD (1998) Neurons in the posterior interposed nucleus of the cerebellum related to vergence and accommodation. I. Steady-state characteristics. J Neurophysiol 79:1255–1269.